Commensurate vortex pinning in Nb films patterned onto anodized aluminum oxide

Wai-Kwong Kwok *, Z.L. Xiao, U. Welp, A. Rydh,
V. Vlasko-Vlasov, V. Novosad

Materials Science Division, Argonne National Laboratory, 9700 S. Cass Ave., Argonne, Il 60439, USA

Abstract

Anodic aluminum oxide templates containing extended arrays of holes with ~ 30-nm diameter and approximately 128-nm spacing were sputter-coated with Nb. We find pronounced matching effects in the transport and magnetization measurements beyond 4 kOe. In addition, we observe Little–Parks oscillations of the superconducting critical temperature. We compare the flux pinning in the patterned samples to unpatterned reference samples and find a significant enhancement of the critical current.
Published by Elsevier B.V.

1. Introduction

The behavior of an ordered array of vortices in type II superconductors superimposed onto an ordered array of pinning sites exhibit a wide range of fascinating fundamental and technological phenomena. The interplay between the vortex–vortex repulsive interaction and the attractive periodic pinning forces generates pronounced commensurability effects [1,2], enhanced critical currents and sharp features in the magneto-transport and magnetization at a characteristic matching field H_1 where the number of vortices equals the number of pinning sites. Furthermore, numerical simulations have predicted the existence of several stable vortex configurations at higher magnetic fields [3]. The existence of these stable vortex configurations have been experimentally demonstrated through Lorentz microscopy [4] and scanning Hall-probe measurements [5].

Generally, the matching fields associated with these experiments have been limited to low magnetic fields (~ 20 Oe) due to the limitations of the lithographic techniques utilized to create the array of pinning sites, i.e. $H_1 \sim \Phi_o/a^2$ where Φ_o is the flux quantum and a is the distance between defects, typically in the range of a micron. Moreover,

---
* Corresponding author. Tel.: +1-630-252-5539; fax: +1-630-252-7777.
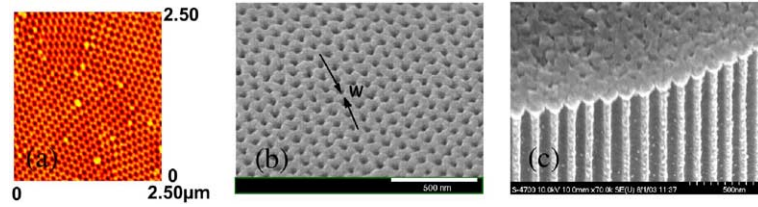*E-mail address:* wkwok@anl.gov (W.-K. Kwok).

Fig. 1. (a) Atomic force microscopy (AFM) image of a section of an AAO membrane. (b) Scanning electron microscopy (SEM) image of a Nb sputtered film on AAO with 45 nm diameter holes and 101 nm period (Film A). (c) SEM image of a cleaved edge of another Nb/AAO film with 30 nm diameter holes and 128 nm period (Film B).

although enhanced pinning is observed in these patterned samples at low temperatures, the commensurability effects are only observed in a narrow temperature range below the superconducting transition temperature, T_c, where pinning and critical currents are generally weak.

Here, we demonstrate a new technique for fabricating laterally patterned superconductors with record small holes and periodicity using a template of anodized aluminum oxide (AAO) membrane. Nb films containing triangular lattices of ~ 35 nm diameter holes with a periodicity of $a \sim 120$ nm over a large area of several cm^2 have been prepared. Due to the comparable size of the hole and the periodicity of the patterned defects to the superconducting coherence length and penetration depth of Nb, we observe pronounced commensurability effects down to liquid He temperature in magnetic fields up to 4 kOe and a large enhancement of the critical current. Furthermore, we observe clear Little–Parks oscillations in the field dependence of T_c.

2. Sample preparation

Anodic aluminum oxide (AAO) membranes were prepared using a two step anodization technique [6]. High purity Al films (99.998%) of thickness 200–500 μm were cleaned in acetone, dried at 100 °C, then baked at 500 °C in an Ar atmosphere to enhance the grain size and subsequently electropolished to a surface roughness of about 10 nm. The films were anodized in an aqueous solution of 0.3 M oxalic acid with various voltages at 0 °C. The first formed layer of AAO is

then stripped away with a mixture of phosphoric and chromic acid and the anodization process is repeated a second time. The AAO nanoporous membranes produced with this technique is highly ordered as shown by the hexagonal array of nanometer sized holes in the atomic force microscopy (AFM) image of Fig. 1(a). Nb films of about 100 nm thickness were sputter-coated on the AAO membrane and capped with a 10 nm Ag layer. Fig. 1(b) and (c) show scanning electron microscopy (SEM) images of two Nb sputtered films on AAO. The first film (A) deposited on AAO anodized at 40 V has a hole diameter of 45 nm with periodicity of 101 nm, yielding a matching field of $H_1 = 2\Phi_o/(3)^{1/2}a^2 = 2255$ Oe [7] and the second film (B) deposited on AAO anodized at 50 V has a hole diameter of ~ 30 nm with periodicity of 128 nm, giving a matching field of $H_1 \sim 1459$ Oe. Note that Film B is not as regular as Film A after Nb sputter coating.

3. Results and discussion

The temperature dependence of the resistance for Film B was measured with the standard ac four probe technique at 23 Hz with a driving current of 10 μA. Fig. 2 shows the superconducting transition at magnetic field cooled intervals of 200 G perpendicular to the film surface. The zero field transition for the Nb/AAO film is about $T_c = 7.5$ K, whereas the transition for a concurrently prepared reference continuous Nb film on a sapphire substrate is 7.7 K. The slight reduction in T_c may be caused by the proximity with the Ag capping layer and by contamination or interdiffusion at the
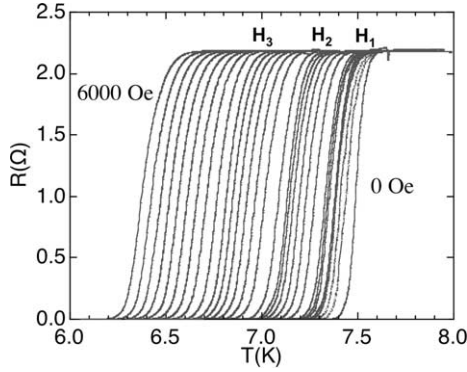
Fig. 2. Temperature dependence of the resistance for Film B taken at magnetic field intervals of 200 G.

Nb–AAO interface. In the presence of a magnetic field, we observe bunching of the superconducting resistive transition curves near integer multiples of the expected matching field $H_1 \sim 1400$ Oe. The shape of the transition is field and current independent and we determined the upper critical field, $H_{c2}(T)$, from the mid-points of the transition curves.

The phase diagram of Film B obtained from the resistive transition curves is shown in Fig. 3. Also shown is the $H_{c2}(T)$ for the reference continuous Nb film. The upper critical field of Film B is characterized by a strong nonlinear temperature dependence near T_c on which an oscillatory variation is superimposed. A linear $H_{c2}(T)$ dependence

is recovered below $T = 6.5$ K. The parabolic dependence of H_{c2} near T_c can be understood in terms of a one dimensional nature of superconductivity when the coherence length, $\xi(T)$, near T_c, becomes larger than the $w \sim 90$ nm width of the Nb section or bridge between the hole arrays. The upper critical field can then be described by the thin film formula, $H_{c2}(T) = (12)^{1/2}\Phi_o/2\pi w \xi(T)$ where $\xi(T) = \xi(0)(1 - T/T_c)^{-1/2}$ [8]. A fit of this expression to our data yields $\xi(0) \sim 18$ nm. This value is significantly smaller than the BCS coherence of $\xi_o = 38$ nm for Nb [9], indicating that our film is in the dirty limit with an electron mean free path of $l = 1.38\xi(0)^2/\xi_o \sim 11$ nm. The Ginzburg–Landau parameter can be estimated using the dirty limit expressions for the penetration depth and the coherence length: $\kappa = 0.72\lambda_L/l \sim 3$, where $\lambda_L = 39$ nm is the London penetration depth of Nb [9]. The oscillatory behavior of the phase boundary is demonstrated in detail in Fig. 4 when plotting the difference between the measured T_c and the fit to the thin film expression. Cusps in ΔT_c at integer multiples of the predicted matching field for a triangular lattice $H_1 = \Phi_o/[0.5(3)^{1/2}a^2] = 1459$ Oe are observed. These cusps are a direct consequence of the fluxoid quantization in a multiply connected superconductor and is identical to those observed in the Little–Parks [10] oscillations of single superconducting loops where the kinetic energy associated with the circulating supercurrents
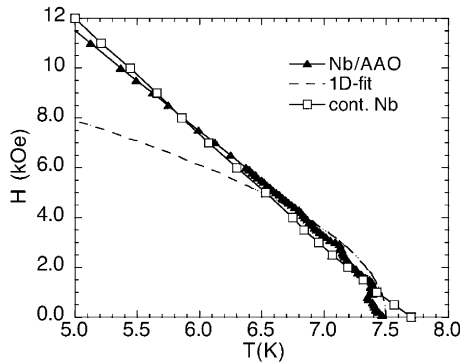

Fig. 3. Superconducting phase diagram of Film B (▲) obtained from the resistive transition curves in Fig. 2. The dashed line is a fit of the data to the one-dimensional thin film formula. Also shown is data on a continuous reference Nb film (□) grown on a sapphire substrate.
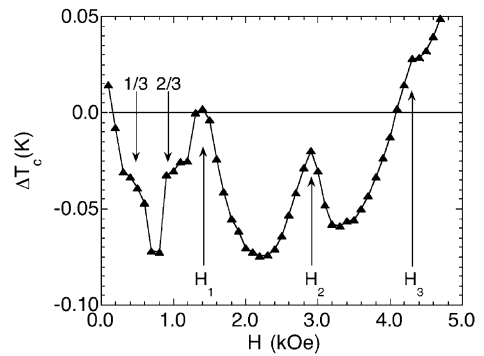

Fig. 4. Oscillatory behavior of the phase boundary plotted as the difference between the measured T_c and the fit to the thin film formula, showing cusps in ΔT_c at fractional and integer multiples of the predicted matching field.

maintaining fluxoid quantization leads to a periodic suppression of T_c. We also observe indications for stable fractional filling factors at $H/H_1 = 1/3$ and $H/H_1 = 2/3$ as expected for a hexagonal array [11].

The field dependence of the width of the magnetization loop of Film B obtained from SQUID magnetometry measurements is shown in Fig. 5 for fields perpendicular to the Nb/AAO surface at several temperatures. We observe pronounced matching effects with cusps at multiple integers of the matching field extending beyond 4 kOe. In contrast to previous reports, matching in our samples is dominant in the magnetization curves even at the lowest temperatures. A comparison with a continuous reference Nb-film (open symbols) indicates a relative increase in the critical current of nearly two orders of magnitude at $T = 6$ K and $H = 3$ kOe.
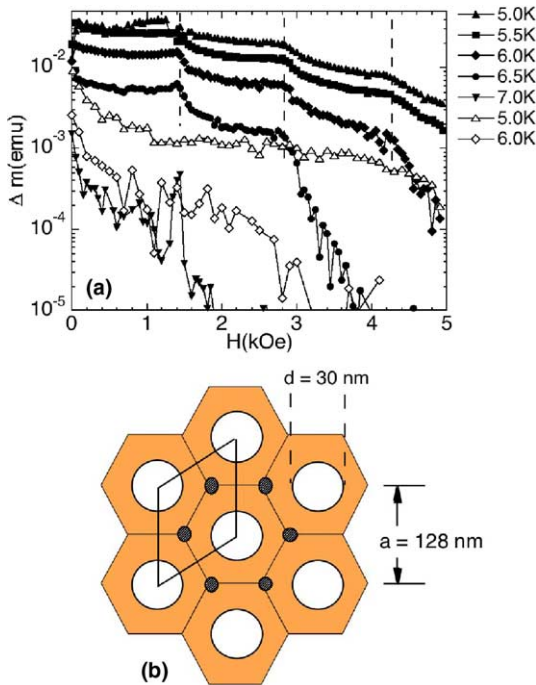

Fig. 5. (a) Field dependence of the width of the magnetization loop of Film B (solid symbols) and of a continuous reference Nb film (open symbols) at several temperatures. (b) Schematic of the Nb/AAO sample with the locations of interstitial vortices.

The matching phenomena above the first matching field can be explained in terms of caging of interstitial vortices between the holes [12] or in terms of multi-quanta vortices trapped in the holes [13]. For a triangular array of holes, doubly quantized vortices are stable for $d^3 > 8\xi a^2$, a condition which is not fulfilled in our sample and indicates the existence of only single-quanta vortices at low temperatures. Furthermore, the attractive pinning force for an isolated hole [14] diminishes if the number of vortices exceeds the saturation number $n_s = d/4\xi(T)$ which is ~ 1 in our samples. As a consequence, when $\xi(T) < w$ at low temperatures, single quanta vortices coexists with interstitial vortices in a stable configuration. The interstitial vortices are pinned by a confining cage potential determined by the ratio $\lambda(T)/a$ and the number of interstitials per unit cell [12]. As $\lambda(T)/a$ decreases with temperature, the confining potential diminishes. However, since in our samples, $\lambda(T)/a \sim 1$, the periodic caging potential is dominant over the entire temperature range. With increasing field, the number of interstitial vortices increases and their interaction energy contributes to decrease the matching effects. We observe matching effects in Film B up to $n = 3$, beyond which the effect is strongly suppressed even at low temperatures. This is consistent with having two interstitial vortices per unit cell as shown in Fig. 5(b).

4. Summary

We have shown that AAO membranes can be used as an ideal platform to create perforated superconducting films with nanosized holes and with nanoscale periodicity extending over large (several cm^2) areas. These Nb/AAO samples have the smallest feature size in extended patterns yet reported and show pronounced commensurability effects over a wide temperature range and enhanced critical currents. The salient feature of these samples is that the coherence length $\xi(0)$ and penetration depth $\lambda(0)$ are comparable to the scale of the periodic pattern, ensuring that the periodic vortex interaction is dominant even at low temperatures.

Acknowledgements

References

[1] A.T. Fiory et al., Appl. Phys. Lett. 32 (1978) 73;
M. Baert et al., Phys. Rev. Lett. 74 (1995) 3269;
V.V. Moshchalkov et al., Phys. Rev. B 57 (1998) 3615;
E. Rosseel et al., Phys. Rev. B 53 (1996) R2983;
A. Castellanos et al., Appl. Phys. Lett. 71 (1997) 962;
V. Metlushko et al., Phys. Rev. 60 (1999) R12585;
L. Van Look et al., Phys. Rev. B 60 (1999) R6998.
[2] J.I. Martin et al., Phys. Rev. Lett. 79 (1997) 1929, 83 (1999) 1022;
D.J. Morgan et al., Phys. Rev. Lett. 80 (1998) 3614;
A. Hoffmann et al., Phys. Rev. B 61 (2000) 6958;
O.M. Stoll et al., Phys. Rev. B 65 (2002) 104518.
[3] Ch. Reichhardt et al., Phys. Rev. B 57 (1998) 7937.
[4] K. Harada et al., Science 274 (1996) 1167.
[5] S. Field et al., Phys. Rev. Lett. 88 (2002) 067003;
A.N. Grigorenko et al., Phys. Rev. Lett. 90 (2003) 237001.
[6] A.J. Yin et al., Appl. Phys. Lett. 79 (2001) 1039;
J. Liang et al., J. Appl. Phys. 91 (2002) 2544;
H. Masuda, H. Fukuda, Science 268 (1995) 1466;
Z.L. Xiao et al., Appl. Phys. Lett. 81 (2002) 2869.
[7] U. Welp et al., Phys. Rev. B 66 (2002) 212507.
[8] M. Tinkham, Introduction to Superconductivity, McGraw-Hill, New York, 1996, Chapter 4.10.
[9] B.W. Maxfield, W.L. McLean, Phys. Rev. 139 (1965) A1515.
[10] R.D. Parks, W.A. Little, Phys. Rev. A 133 (1964) 97.
[11] Ch. Reichhardt, N. Grønbech-Jensen, Phys. Rev. B 63 (2001) 054510.
[12] I.B. Khalfin, B. Ya Shapiro, Physica C 207 (1993) 359.
[13] A.I. Buzdin, Phys. Rev. B 47 (1993) 11416.
[14] G.S. Mkrtchyan, V.V. Shmidt, Zh. Eksp. Teor. Fiz. 61 (1971) 367, Sov. Phys. JETP 34 (1972) 195.